Invited Paper

Tunable terahertz metamaterials

H. Tanoto, L. Ding, and J. H. Teng *
Institute of Materials Research and Engineering
Agency for Science, Technology and Research (A*STAR)
3 Research Link, Singapore 117602
* Email: jh-teng@imre.a-star.edu.sg

(Received January 2, 2013)

Abstract: The adoption of metamaterials in the development of key terahertz (THz) components has led to tremendous theoretical and technological progress in the THz field. This Review discusses the methods and current progresses in tunable THz metamaterials, offering a glimpse of the future applications of these novel devices.

Keywords: Terahertz metamaterials, Terahertz devices, Tunable metamaterials, Metadevices

doi: 10.11906/TST.001-025.2013.03.01

1. Introduction

It took more than 30 years from the theoretical elaboration of negative refractive index [1] to practical demonstration of such characteristics by a kind of structured materials, or metamaterials [2-6]. Now, just slightly over a decade later, metamaterials have become one of the most sought-after scientific research topics, with around ten thousands research publications since year 2000. Due to their unique properties in interacting with electromagnetic waves, metamaterials hold promises in realizing technologies unachievable by natural materials. The last decade of research in metamaterials had reiterated the importance and novelty of such structures, with breakthroughs in both theoretical and experimental fronts and the emergence of many new devices. Metamaterials are typically composed of many metallic individual elements of deep sub-wavelength sizes, such as split ring resonators (SRRs) [2, 7-13], metal-wires [14-17], fishnet structures [18-27], and others. The metamaterials electromagnetic properties are derived from these subwavelength metamolecules, basically resonator elements, encapsulated within dielectric materials. The metamolecules are akin to atoms or molecules in natural materials. Although the composing materials do influence the metamaterials properties, the metamolecules' configuration remains the dominating factor. The precise shape, geometry, size, orientation and arrangement of the metamolecules dictate the amplitude, direction, polarization, wavelength, and phase of electromagnetic waves interacting with the metamaterials. As such, one can see almost unrestrained flexibility in designing the elements in the metamaterials to produce wide gamut of

electromagnetic properties [4, 6]. Through clever design of the metamolecules, metamaterials have demonstrated exotic properties and possibilities such as negative refraction [7, 8, 13], [28-33], perfect absorption [34-37], super lens effect [38-49], transformation optics [50-56], chirality [28, 57-60], and many more.

The applications of terahertz (THz) waves are wide-ranging, from security screening, medical imaging, wireless communications, non-destructive evaluation, chemical identification, and others [61-80]. Due to their low photon energy, THz waves do not ionized biological cells and thus are much safer for human inspections, unlike using X-rays. In astrophysics and earth sciences, thermal emission for a wide variety of light weight molecules is specifically amenable to THz band. In fact, the universe is bathed in THz energy with most of it remain unnoticed and undetected [81, 82]. Just over two decades ago, however, the region between 0.1-10 *THz* was called 'THz-gap' due to the lack of efficient components like source, detector, modulator, waveguides and filters [83]. Conventional transmissive optical materials from which lenses or other traditional optical devices are made typically suffer high-loss when operating at the THz range.

Immediately following demonstration of metamaterials in microwave region [5, 84, 85], scientists have moved on adopting such structures in THz research and many THz metamaterials and devices have been developed, such as absorbers, lenses, switches, modulators, sensors, as well as phase-shifting and beam-steering devices to control and manipulate THz waves [12, 86-93]. To extend the operation bandwidth of metamaterials, or to have the devices actively responding to the need of the systems and adjust their operation frequency, active tunability of metamaterials response is needed. The tunable metamaterial devices can enhance the functionality and flexibility of the THz systems. This paper will review tunable THz metamaterials based on various technologies, including electro-mechanical, thermo-mechanical, magneto-mechanical, electro-optical and finally, through altering the shape of the substrate or flexible metamaterials.

2. Electro-mechanical THz metamaterials

Microelectromechanical system (MEMS) has been extensively used in many applications [94-104], and its applicability in THz metamaterials was first applied in tuning the transmission lines [105-109]. By using MEMS-based processes to fabricate platform structures to control the spacing and configuration of the resonant element [110, 111], electro-mechanical mechanism was used to control the shape and configuration of the resonant components of metamaterials in real-time. One important advantage of using silicon based MEMS is its CMOS compatible fabrication process for potential low cost large volume manufacturing.

Real-time tuning of the THz magnetic response of metamaterials has been derived from reshaping the metamaterial elements. Figures 1 [111] shows a micromachined metamaterial, consisted of 400 × 400 split ring resonators (footprint 10.8 *mm* × 10.8 *mm*), fabricated by using the silicon micromachining technology. The metamaterial element employs two identical electrostatic comb-drive actuators on both sides for mechanically balanced translation. Each comb-drive actuator provides bidirectional, in-plane translation. The geometry of the structurally reconfigurable metamaterial elements changes from close-ring state ('□' shape) to open-ring state ('[ ]' shape), and back-touch state ("I" shape). Simulation results of the induced surface currents by the magnetic response under the TE polarized incidence show the surface currents of the three states are concentrated on the metal parts, which suggests that the magnetic response of each metamaterial molecule is controlled by the shape and coupling of the metal parts. In the open-ring state, Fig. 1(a), the directions of the surface currents on the two split rings form a loop so that the induced magnetic fields point in the same direction, causing a strong magnetic response to the incident magnetic field. Such magnetic response could be strong enough to overcome the incident magnetic field, effectively resulting in a negative magnetic response. In contrast, in the closed-ring state, Fig. 1(b), and the back-touch state, Fig. 1(c), the surface current directions of the two split rings are in opposition to each other and cause a poor magnetic response. Such responses are verified in the reflection spectra. The fabricated structures are shown in Fig. 1(d) with close-up view in the inset. The experimental observations show clearly that the switchable magnetic metamaterial can be changed from a magnetic metamaterial to a non-magnetic metamaterial by reshaping the metamaterial molecules. Figure 1(e) is the effective permeability, μ, as derived from the measured spectra using the Fresnel fitting method. With a gap of 2 *μm*, a tuning of the permeability from negative (–0.26) to positive (0.29) near the resonant frequency around 2 *THz* is achieved.

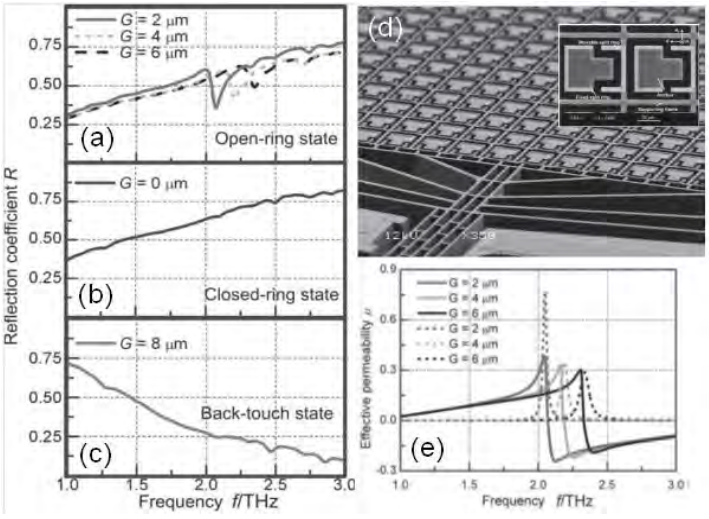

Fig. 1 The measured reflection coefficient R of the metamaterial under the TE polarized incidence. a) The open-ring state (G = 2 *ìm*, 4 *ìm*, and 6 *ìm*), b) the closed-ring state, and c) the back-touch state. (d) SEM image of the micromachined switchable magnetic metamaterial, inset: a zoom-in view of the metamolecule. (e) The effective permeability. The solid and the dotted lines represent the real and the imaginary parts of the effective permeability, respectively. (Copyright © 2011 WILEY-VCH Verlag GmbH & Co. KGaA, Weinheim)

Figure 2 shows the reconfigurable THz metamaterial reported to realize a dual mode resonance switching in THz region [112]. The sample consists of a 200×200 element array which has an in-plane translational period of 60 μm as shown in Fig. 2(a). The metamaterial element was formed by patterning an evaporated aluminum layer on the top of Si structures. The supporting frame is connected to the micromachined comb drive actuator which provides bidirectional in-plane translation up to 30 μm driven by the electrostatic force. CLOSE-state and OPEN-state are shown in Fig. 2(b), top and bottom, respectively. The measured reflection spectra as measured in oblique incident conditions are shown in Figs. 2(c) and 2(d). When Ö = 0°, dual mode resonance is observed at 0.76 *THz* and 1.16 *THz* in the CLOSE-state and vanishes as the metamaterial is switched to the OPEN-state. The reflection relative ratio is 59% and 34% at the two frequencies, indicating that a dual mode resonance switching is realized through the metamaterial element reconfiguration. The resonance at 0.76 THz is observed in the metamaterial CLOSE-state when Ö = 90°. The reflection relative ratio reaches 67% at 0.76 *THz* while keeps below 30% at other frequencies from 0.73 *THz* to 1.23 *THz*. The resonance switching function enables wide applications of the metamaterial in modulators, switches, tunable filters, and THz detectors.

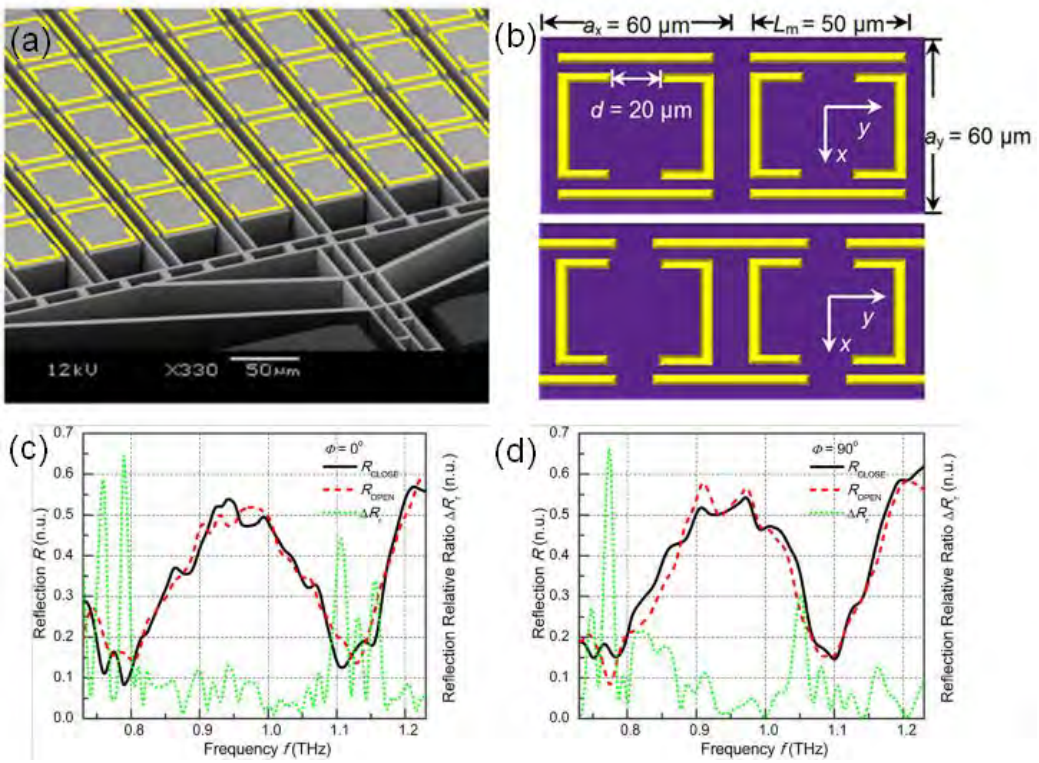

Fig. 2 (a) SEM images of the metamaterial structure in [112]. (b) Top schematic view of two elements in the CLOSE-state (top) and the OPEN-state (bottom). The reflection spectra under TE polarization in the CLOSE-state (dash) and the OPEN-state (solid) of the metamaterial when Φ is (c) 0° and (d) 90°. Dotted line: the reflection relative ratio ΔR_r. (Reprinted with permission from [112]. Copyright [2012], American Institute of Physics.)

The tuning capabilities of metamaterials can also be realized from changes in near-field coupling, obtained through in-plane displacement of the two SRR layers [110]. The structures were fabricated using MEMS compatible processes. The two layers of SRR structures are sandwiched between two layers of polyimide deposited on a substrate. They were then removed resulting in a thin metamaterial film with a thickness of 14 ìm. The tuning of THz responses of the metamaterials was obtained by lateral shifting of the SRR layers under electrical excitation. Optical micrographs of the shifted arrays are shown in Fig. 3(a) with the corresponding simulation and experimental results in Figs. 3(b) and 3(c), respectively. The resonance frequency decreases from ~1.35 to ~0.63 *THz* as the displacement increases, which means tuning of 51%. These features provide the reconfigurable metamaterials with a unique merit of widely tuning the THz electromagnetic response.

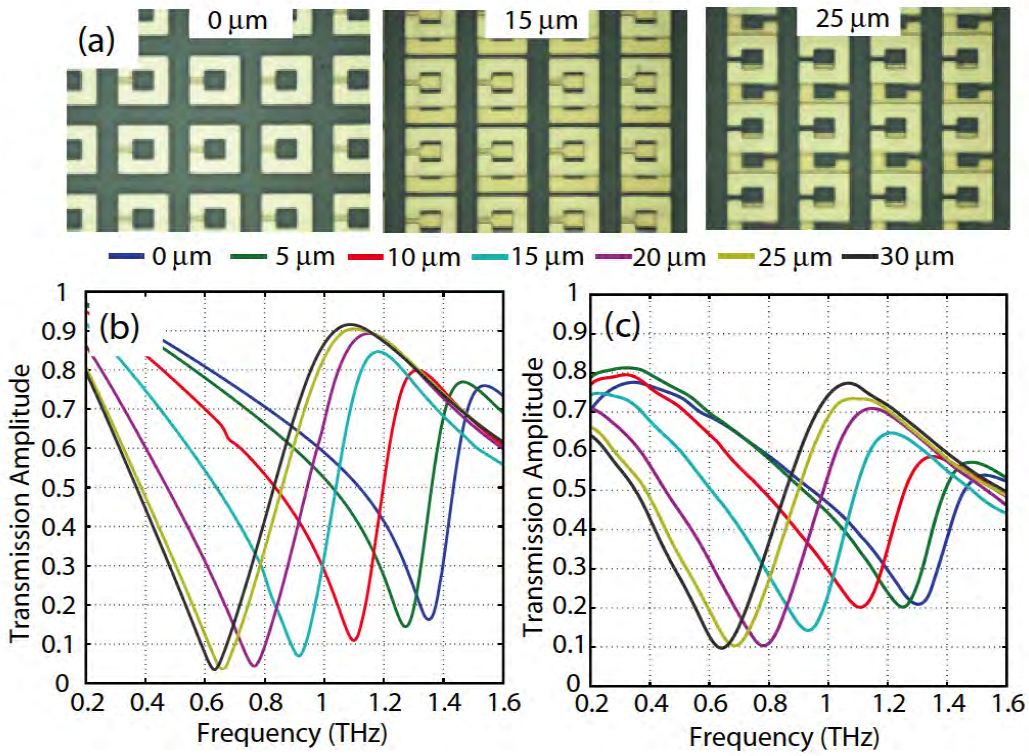

Fig. 3 (a) Optical micrographes of SRR structures shifted along the vertical direction for 0 (no shift), 15, and 25 *ìm*. (b) Simulation and (c) measurement results for THz transmission characteristics of the SRR structures shifted along the vertical direction for 0, 5, 10, 15, 20, 25, and 30 *ìm*. (Copyright to be applied)

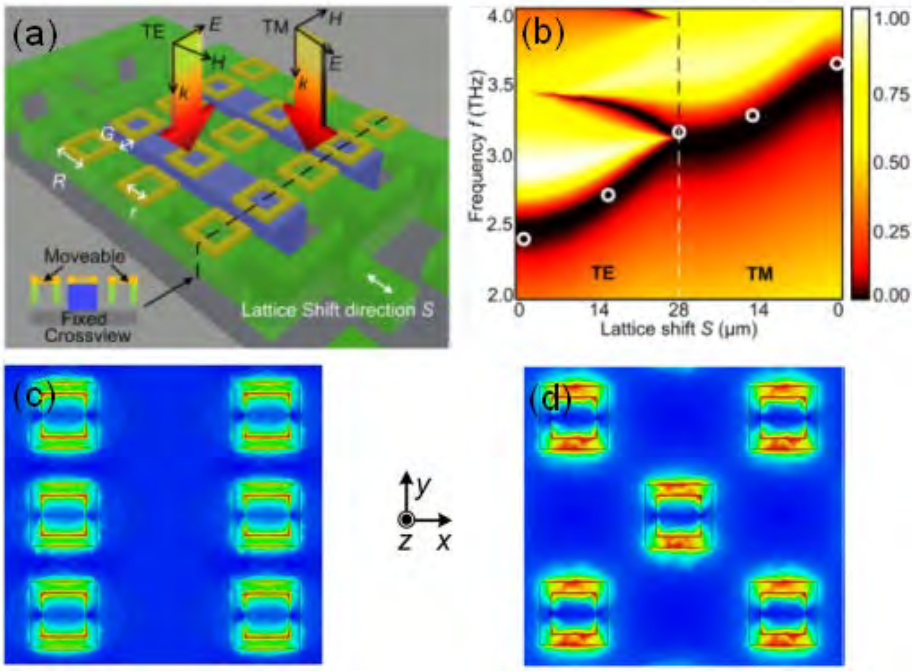

Fig. 4 (a) A schematic of the THz micro-ring metamaterial. The movable rings are located on the released part of the silicon frame which is actuated by the comb drive actuator along the *x* direction. The fixed rings are patterned on the insolated silicon islands which are anchored on the substrate. (b) Contour map of transmission coefficient for TE (left sided) and TM (right sided) polarized incidences. The bright region shows the high transmission region while the dark region shows the transmission dip. The transmission spectra of both TE and TM polarized light are numerically analyzed under the lattice shift from 0 μm to 28 *μm*. The transmission spectrum becomes polarization independent when the lattice shift is 28 *μm* which is proved by the continuity of the contour map at the interface (marked by white dashed line). The white circles represent the transmission dips measured in experiment which show a good agreement with the simulation results. (c) and (d) The cross view of the THz micro-ring metamaterial shows the lattice pattern when the lattice shift S = 0 *μm* and S = 28 *μm*, respectively. The color represents the intensity of the surface current induced by the TE polarized light at frequency 3.11 *THz*. (Reprinted with permission from [113]. Copyright [2011], American Institute of Physics.

In Ref. [113], a polarization dependent state to polarization independent state change in THz metamaterials was accomplished by reconfiguring the lattice structure of metamaterials from twofold to fourfold rotational symmetry by using micromachined actuators as shown in Fig. 4(a). A contour map, seen in Fig. 4(b), shows the resonance frequency shift of 25.8% and 12.1% for TE and TM polarized incidence, respectively, by shifting the lattice from 0 *μm* to 28 *μm*. Furthermore, single-band to dual-band switching is also demonstrated. Figures 4(c) and 4(d) show the lattice pattern when the lattice shift S = 0 *μm* and S = 28 *μm*, respectively. The color represents the intensity of the surface current induced by the TE polarized light at frequency 3.11 *THz*. The lattice reconfigurable metamaterials promises a strong engineered optical anisotropy with large tuning capabilities in THz region, which can be used in the photonic devices such as sensors, optical switches and filters.

Recently, MEMS process was also used to realize tunable anisotropic THz metamaterials based on Maltese-cross pattern [114]. The fabricated structures are shown in Figs. 5 (a) and 5(b). The wide-range tuning from positive anisotropy to negative anisotropy was achieved. The anisotropy is induced through breaking the four-fold symmetry of the cross by changing the position of one of the beams. The breaking of the Maltese-cross symmetry leads to the change in the resonance modes of the e-polarized incidence. On the other hand, the o-polarized incidence is only altered slightly. Large tunability of optical anisotropy at 3.0 *THz* and 4.6 *THz* incidence is observed either at 0 μm < S < 1 μm or 4 μm < S < 5 μm, as shown in Figs. 5(c) and 5(d). The optical anisotropy is changed abruptly, when the movable beam is disconnected from the fixed ones. This device may be applicable in the development of terahertz variable waveplates, tunable filters and polarimeter.

Thus far, MEMS technology has proven to be a promising method to realize reconfigurable and switchable metamaterials in addition to offering more freedom for metamaterial design resulting in larger tunability and easier fabrication. With the typical period of the micromachined metamaterial element in tens of micrometers, they are ideally suited for working frequency in THz region. However, with response time in hundreds of microseconds, micromachined metamaterials are only suitable in applications where high speed modulation is not essential. Further developments in nanoelectromechanical systems will lead to more efficient designs, more compact structures, and higher operating frequency.

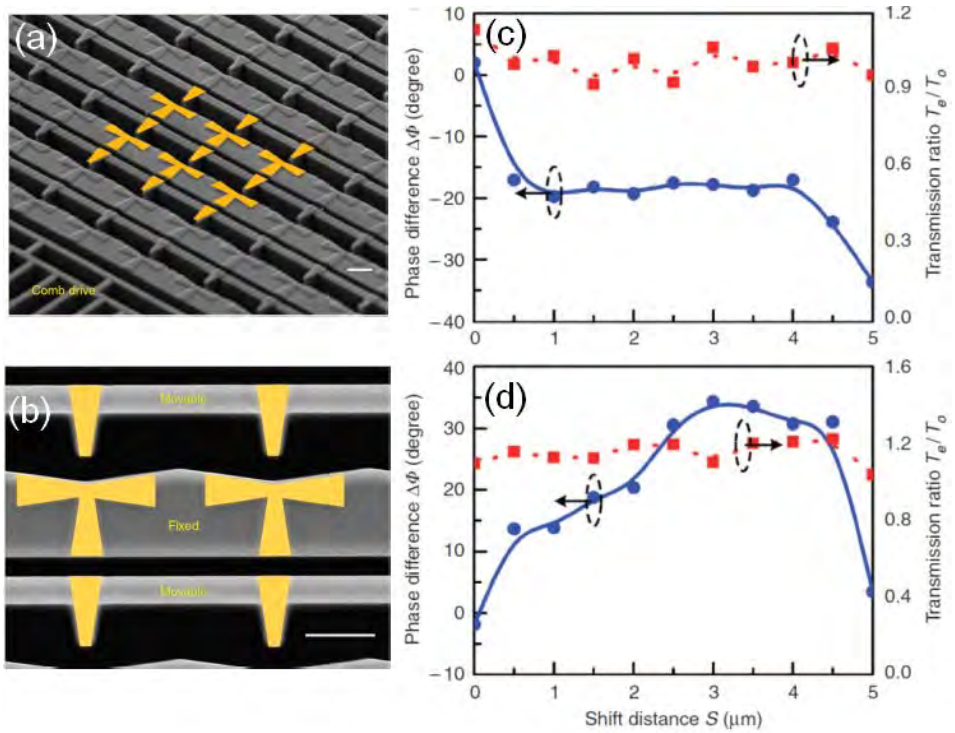

Fig. 5 anisotropic metamaterials based on Maltese-cross pattern (a) whole structure, (b) side view of metamolecules. The differential phase retardation and transmitted power ratio for (c) e- and (d) o-polarized light as functions of the shift distance. (Copyright needs to be applied by publisher)

3. Thermo-mechanical and magneto-mechanical THz metamaterials

Thermal tuning of metamaterials electromagnetic response by relying on the difference in the thermal expansion between metal elements and the surrounding matrix materials is also a promising approach. It enables reconfigurability with simple fabrication. In one design, the difference in thermal expansion coefficient of metal and semiconductor/dielectric is such that a change in temperature leads to a bending of a bi-material cantilever. Considering a few microns' actuation or less, thermal heating is efficient in terms of the power consumption, which makes it very useful to realize thermo-mechanical tunable metamaterials working in the THz region or beyond.

Figure 6 shows two recent researches on THz thermo-mechanical tunable metamaterials [92, 116]. Figure 6(a) depicts a SRR unit cell along with two bi-material cantilever legs [92]. The electromagnetic response is a sensitive function of orientation. At normal incident THz waves, the tunable metamaterials do not have resonant response when the SRRs lie in the plane of the substrate. When the cantilevers bend upwards with increasing temperature, the magnetic field can penetrate through the SRRs and drive the magnetic resonance. The insets show the SEM pictures of the fabricated bi-material cantilever metamaterials lying in-plane and bent upwards out of the plane of the substrate at different temperatures. More complex structures could be designed where a fraction of the unit cells remain stationary or different unit cells move in orthogonal directions [116], as shown in Figures 6(b) and 6(c). These results highlight the possibility of creating reconfigurable metamaterials potentially leading to dynamically reversible refractive index structures or thermal detectors amongst other possibilities.

Theoretical work has also been carried out on the magneto-mechanical tunable THz metamaterials [117]. The micromachined cantilevers used to tune the metamaterial are actuated by the force generated by an external field on the magnetic material coating on the surface. The use of cantilevers enables continuous tuning of the resonance frequency over a large frequency range. The proposed tunable metamaterial has field induced nonlinearity, which is possible to be realized using current micromachining technologies. Magnetic actuation of single end fixed cantilevers in micromachined devices has been studied and demonstrated before [118, 119]. In addition to translation, the magneto-mechanical actuators can be used to rotate the micromachined structures. This may be useful in making micromachined tunable metamaterials with rotational metamaterial elements.

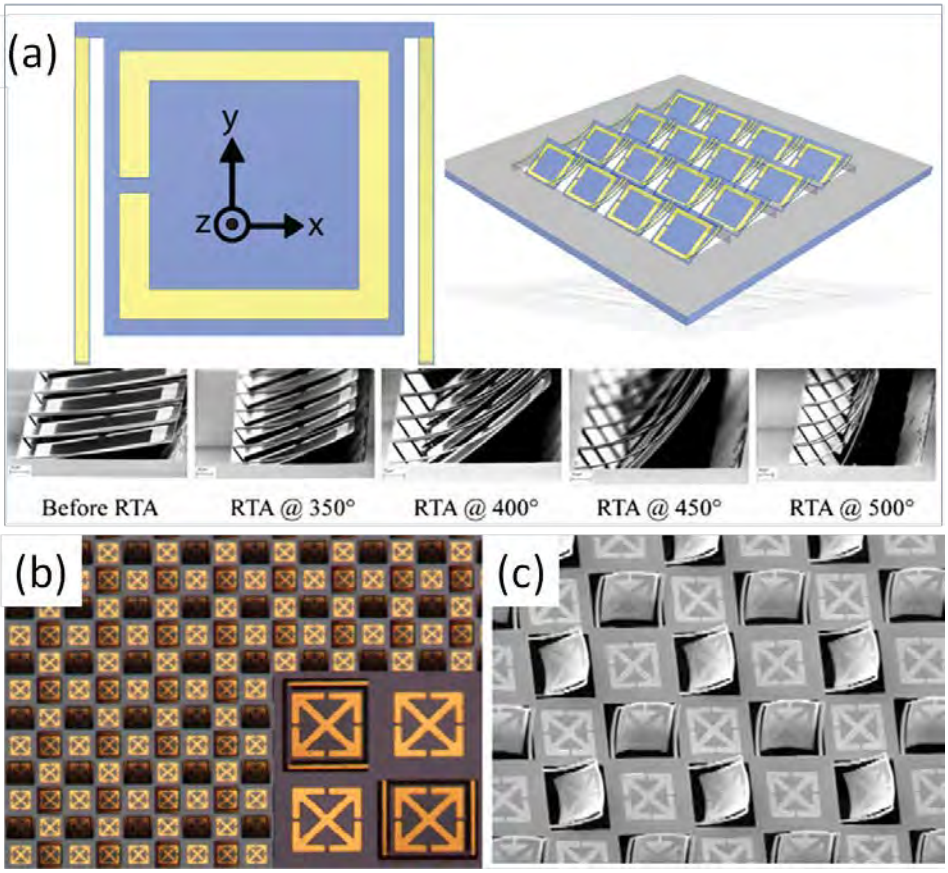

Fig. 6 Schematic diagrams of tunable THz metamaterials via thermo-mechanical bending of the metamaterial elements. (a) Unit cell consisting of a split ring resonator and cantilever legs. Schematic view of a portion of the metamaterial structure highlighting how the SRRs rotate as the cantilever legs bend. Inset is SEM pictures showing the bending of the SRRs at different temperature. (b) A metamaterial structure with different unit cells remaining stationary or moving in orthogonal directions, (Inset) Zoom in picture. (c) SEM photograph of the same sample after selectively rotating different elements out of the plane. (copyright need to be applied by publisher)

4. Electro-Optical THz metamaterials

One of the important steps in metamaterials technological development for industry adoption is the integration with the highly established semiconductor technology. To achieve tunability, the metamolecules are deposited on the surface of photo-sensitive semiconductors, using photo-induced conductivity phenomena to tune the metamaterials electromagnetic characteristics. This method was used to control mode switching and showed a broad blueshift tuning range of 40% [120]. The unit cell consists of conducting silicon within the two side gaps of the LC resonator on sapphire. When illuminated, the silicon becomes highly conductive and thus, changing the unit cell LC response. The field and current distributions of the non-illuminated cell and illuminated cell display the distinct modes.

Employing semiconductor electric diode device, novel planar electric metamaterials operating at THz frequencies was also demonstrated [121]. The terahertz transmission modulation of 50% was achievable. Gold metamolecules fabricated on a GaAs substrate effectively formed Schottky diode. Illustration of the device is shown in Fig. 7(a), with inset showing the metamolecule. The conductivity, and thus dielectric properties, of the substrate is again controlled through photo-excitation. Applying voltage bias to the metamolecules changed the THz conductivity of the substrate underneath and surrounding the metamolecules, resulting in varied resonance. Figures 7(b) and 7(c) show the THz time-domain signal and frequency spectra, respectively, at various modulation frequencies. It can be seen that the peak of the spectrum lies at 0.46 *THz* indicating modulation of the metamaterial resonance. Bandwidth of the spectra remains relatively unchanged between 100 *kHz* and 1 *MHz*, while the amplitude increases. An array of 4 × 4 *pixels* voltage-controlled room-temperature THz modulator was also developed using similar technique. Each pixel consists of SRR elements independently controlled by applying a small external voltage with low overall power consumption. The modulator showed modulation depth of around 40% with very low crosstalk [122]. Similar hybrid-metal-semiconductor SRRs were also employed in demonstrating THz metamaterial absorber. Tuning the response by external pump power, an effective control of the absorption strength and peak frequency was shown [123]. A broadband tunability of the absorption peak frequency was observed, varying from 1.11 to 0.87 *THz*, while achieving 60.5% of the amplitude modulation depth. The performance was derived from tuning of the silicon reflection by photo-induced conductivity.

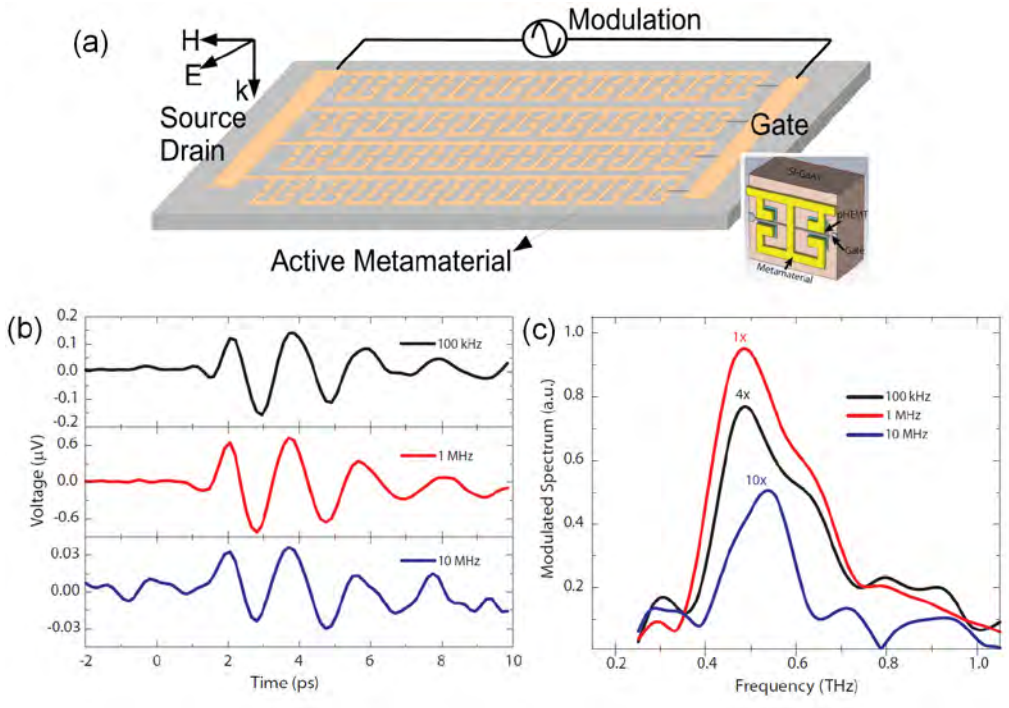

Fig. 7 (a) Active metamaterials hybrid Schottky diode, with inset showing the metamolecule. (b) and (c) show the THz time-domain signal and frequency spectra, respectively, at various modulation frequencies. (copyright to be applied)

So far most of the metamaterials devices in THz range are made of the combination of noble metal and dielectric materials. Unlike in the visible frequency, noble metal is almost a perfect conductor in THz range without surface plasmon characteristics, which can provide more design flexibility and special interesting phenomena. Surface plasmon effect in THz range can be generated either through surface structured metals to get so-called spoof surface plasmon [124-126], or by using semiconductor materials, which are more versatile in terms of tuning the plasmon properties and forming active THz plasmonic metamaterials and devices. With its small effective mass and high electron mobility, InSb is a very good candidate for plasmonic materials at THz range [127, 128]. It has been used to demonstrate broadband absorption in THz range by using InSb touching disks to prove a transformation optics design for light harvesting using gold nanostructures at visible frequencies [129]. By directly modulate the plasmonic properties of InSb, a direct optical tuning of the THz response in an InSb based subwavelength grating structure was demonstrated recently [130]. The subwavelength InSb grating structure was fabricated on a 2-*μm*-thick InSb on semi-insulating GaAs substrate, with a period of 4 *μm*. Figures 8(a) and 8(b) show the SEM images of the fabricated InSb grating. Transmission of THz waves through the subwavelength grating under optical excitation is schematically shown in Fig. 8(c), where a polarized incident THz wave is shinning normally onto the sample and a 405 *nm* wavelength laser beam with an incident angle of ~ 45° is used to optically pump the sample.

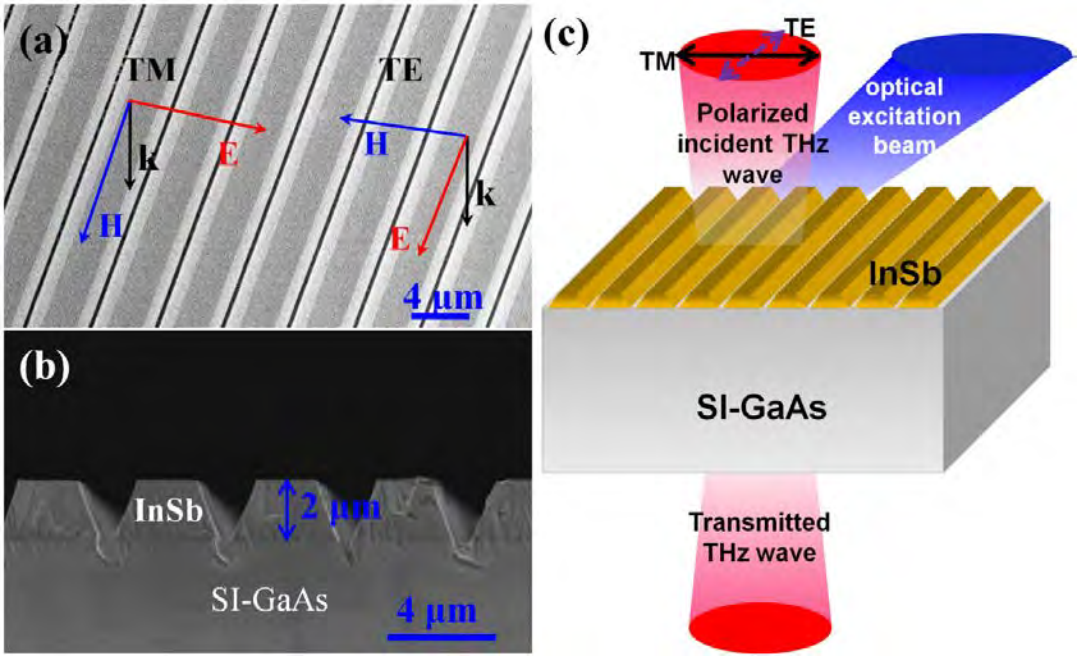

Fig. 8 (copyright to be applied) Scanning electron microscope (SEM) images of the fabricated InSb grating viewed from (a) top and (b) cross section. (c) Schematic of the transmission measurement configuration used in FTIR. The 405 *nm c.w.* laser is shone onto the InSb grating at an incident angle of ~ 45°. Electric and magnetic field configurations of normally incident TE and TM waves are indicated in (a). H: magnetic field; E: electric field

The transmittance of TM and TE polarized THz waves through the InSb subwavelength grating with/without 405 *nm* laser excitation are characterized using Fourier-transform infrared spectroscopy (FTIR) as shown in Fig. 9. The laser excitation generated extra free carriers in InSb and increased electron concentration, which in turn resulted in an increase in plasma frequency and hence the localized surface plasmon resonance frequency in the trapezoid grating array. As shown by the red curve in Fig. 9(a), the transmittance minimum of TM wave shifts from 1.3 *THz* to 1.5 *THz* after laser excitation. The transmittance at 1.5 *THz* decreases from 0.6 to 0.32, a change of 46.7%. On the other hand, for TE polarization, a transmission change is hardly observable. A modulation response speed up to 1.2 *GHz* was characterized using optical pumping THz probe (OPTP) spectroscopy. Numerical calculation reveals wide tunability of this modulator by optical excitation in terms of both modulation frequency and depth. The direct all optical tuning and modulation of the plasmonic response of InSb provides many flexibilities and new possibilities in future THz metamaterials and THz component development.

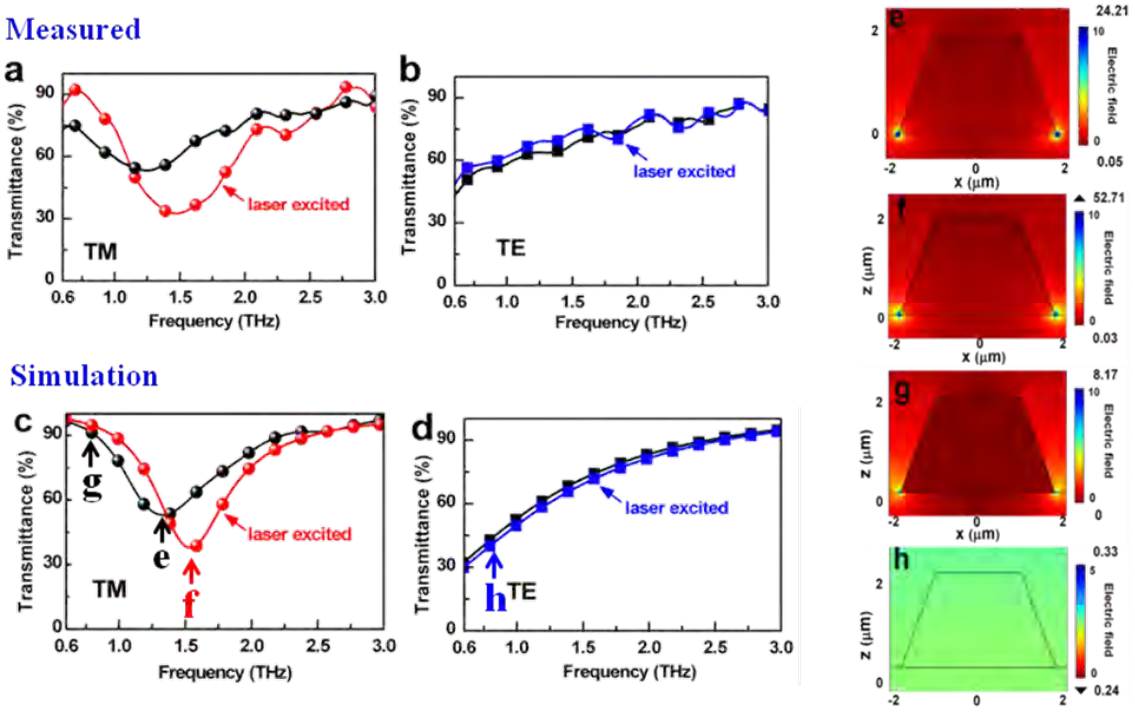

Fig. 9 Measured transmittances of (a) TM and (b) TE polarized THz waves through samples without and with laser excitations. (c) and (d) are the corresponding simulated transmittances. (e) ~ (h): Electric field patterns under different conditions calculated by FEM. (e): TM at 1.3 *THz* without laser excitation; (f): TM at 1.5 *THz* with laser excitation; (g): TM at 0.7 *THz* without laser excitation; (h): TE at 0.7 *THz* without laser excitation. The maximum values of electric fields are indicated at the top of intensity bar. (copyright to be applied)

Graphene, a two dimensional materials with only one atom thick, has attracted extensive attentions since the practical production of stable graphene in 2004 [131]. Various electronic and optical effects have been found in graphene such as integer and fractional quantum Hall effect at room temperature, tunable band gap, ballistic electronic propagation, optical saturable absorption

and luminescence [132, 133]. Graphene manifests strong absorption of light in the near-infrared and visible range, while at mid-IR and THz range the intraband transition of electrons dominates and graphene behaves like a metal, which can support transverse magnetic (TM) polarized surface plasmon polaritons (SPPs) and becomes a good candidate for plasmonic metamaterials [131, 134, 135]. The large modal index, relative low loss and especially the tunability by electromagtic field and gate voltage on its plasmonic properties make it very suitable for tunable metamaterials and meta-device applications [136, 137]. A tunable graphene microribbon THz modulator operating based on electro-optical effect was recently demonstrated, as shown in Fig. 10 [136]. It was found that the ribbon width and carrier doping affect the plasmon frequency with characteristics of two-dimensional massless Dirac Fermions. The tunability of graphene through gating is attractive for modifying the electromagnetic response of the metamaterials.

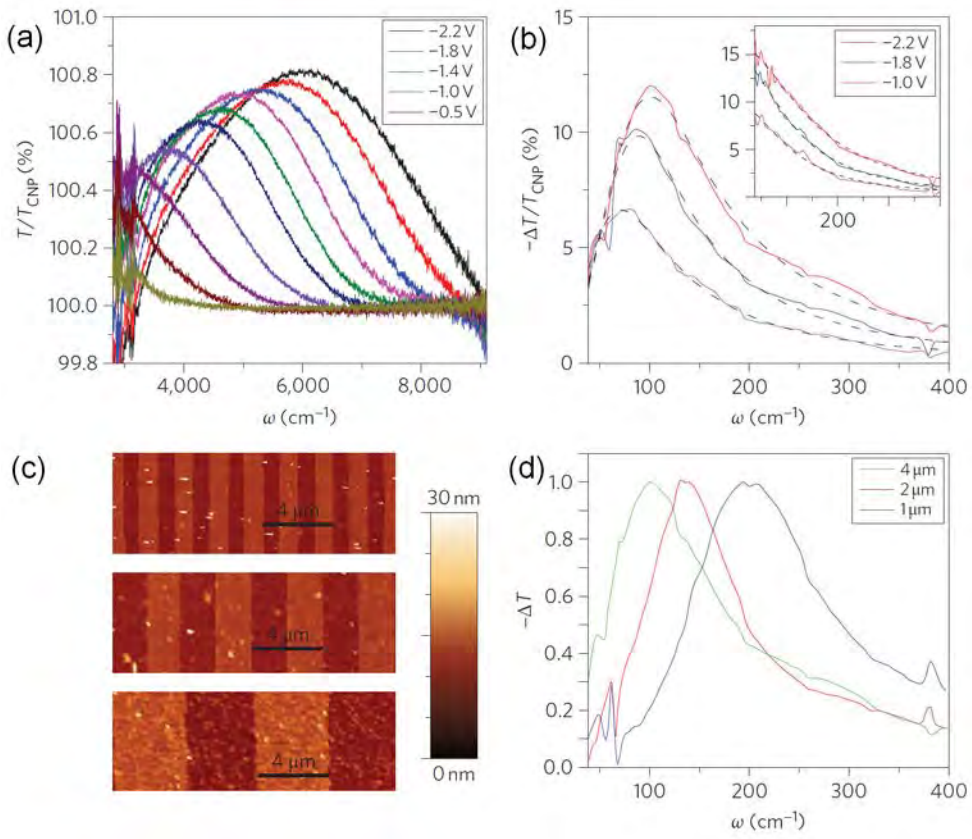

Fig. 10 Control of plasmon resonance through electrical gating and micro-ribbon width. (a) Mid-infrared transmission spectra as functions of gate voltage. (b) Terahertz resonance of plasmon excitations by electrical gating with THz radiation perpendicularly polarized to the graphene ribbons. (c) AFM images of samples with micro-ribbon widths of 1, 2 and 4 μm. (d) Transmission spectra with different graphene micro-ribbon widths. (Reprinted by permission from Macmillan Publishers Ltd: [Nature Nanotechnology], copyright (2011))

With large oscillator strengths in its plasmon resonances, graphene can induce strong room-temperature optical absorption peaks. This can be further amplified over broad THz frequency by

using in-situ electrostatic doping. To further improve the electro-optic tunability of graphene metamaterials, the atomically-thin graphene layer is integrated into hexagonal-patterned metamolecules sandwiched by dielectric layers [138], as shown in Fig. 11. A substantial gate-induced persistent switching and linear modulation of terahertz waves was achieved. The strong resonances of the metamaterials also enhanced the gating controlled electromagnetic properties of graphene. In total, both effects resulted in 47% amplitude modulation of THz transmission and 32:1phase modulation at room temperature.

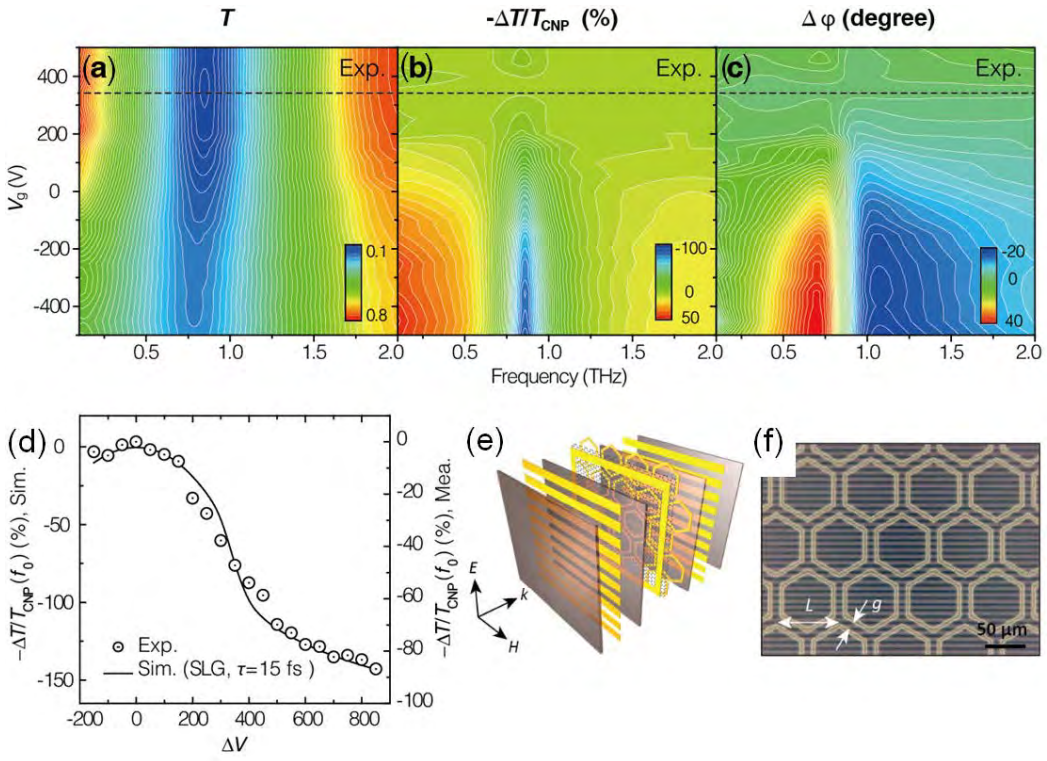

Fig. 11 Gate-controlled amplitude and phase changes of THz waves transmission through the graphene metamaterials, measured spectra of (a) transmission, (b) relative change in transmission, (c) phase change, all plotted as a function of gate voltages. (d) The relative change in transmission at a resonance frequency of 0.86 *THz*, scatters and solid are for the experimental and simulation, respectively. (e) and (f) schematic of the metamaterial device and optical micrograph of graphene metamaterials, respectively. (Reprinted by permission from Macmillan Publishers Ltd: [Nature Materials], copyright (2012)

Despite great progress in electro-optical materials and device research, fast, efficient and small active elements are still difficult to achieve. With metamaterials, fast and deep modulation can be achieved with low power consumption and subwavelength layer thickness or even atomic thickness of graphene. This is the main competitive advantage of metamaterials over traditional electro-optical crystals technology.

5. Flexible THz metamaterials

Fabricating metamaterials on flexible substrates with much thinner dimension than the metamolecules dimensions, one can easily get tunable properties through the structural change of the substrate, or get three-dimensional metamaterials by stacking or rolling the film. Naturally, due to the flexibility, the flexible metamaterials can be coated on non-planar surfaces for shielding, concentrator or absorber applications. Polyimide substrates as thin as 5.5 μm has been employed to demonstrate free-standing metamaterials [139]. The devices were found to exhibit strong robustness with no degradation of properties even after rinsing in organic methanol and isopropanol, tearing and tweaking, and heating up to 350°*C*. Quasi-three-dimensional THz electric metamaterials were then demonstrated on this substrate. From the transmission characteristics obtained through TDS, they show non-dependency between effective dielectric function and the number of layers. In addition, it was found that by decreasing the thickness of the polyimide substrates, the metamaterials show negative dielectric response.

Terahertz metamaterials were also fabricated on polydimethylsiloxane (PDMS) substrate, by which the cost, inertness and ease of fabrication are its main advantages. PDMS is also widely used in microfluidics, allowing potential metamaterials-microfluidics hybrid device development. Flexible fishnet THz metamaterials was fabricated on 250 μm thick PDMS substrate. Alternating layers of chromium (20 *nm*) and gold (200 *nm*) were used to minimize film stress and to improve adhesion [140]. A thin layer of PDMS (10 μm) is used to isolate two fishnet layers. Five layers fishnet structure were obtained after repeated process. Fig. 12(a) shows the simulated and measured THz response of the five-layer fishnet metamaterials, with inset showing the device structures. Measurement results showed resonant dips at 2.0 *THz* and 2.1 *THz* and evidence of splitting in the high transmission area after the resonant frequency.

Metamaterial tubes made of solid semiconductor materials were also found to exhibit unique THz properties. The semiconductor layers relax their strain upon release from the substrate by rolling up into microtubes similar to a rolled-up carpet. Strictly speaking, it is not a flexible metamaterials, but the fabrication process does involve the elastic characteristics of semiconductor layer, so we include the discussion in this section. For optical metamaterials fabrication, the walls of rolled-up structures are treated as metamolecules, but for THz frequency, the entire rolled-up structure is treated as a unit cell. Strong chiral properties were observed from an array of (In)GaAs/GaAs/Ti/Au microhelices of 11 μm in diameter and 52-53 degree helix angle [141]. Due to strong preferential rolling direction of self-rolling layers in the InGaAs materials, a well-defined angle can be realized. Circular dichroism and polarization rotation around 2 *THz* were found. Figure 12(b) shows simulated transmission spectra of microroll arrays with varying winding numbers, the inset show THz metamaterials made of array of rolled-up InGaAs/GaAs/Cr microtubes. These structures have more than one rotation and analogue to SRR. The magnetic response is dependent on the number of rotation. A negative permeability is

achievable when the rotation extends beyond one rotation and the resonance frequency can be approximated by a simple Lorentz-oscillator model.

Tuning of the resonant peak was also found by rolling the THz metamaterials into tube-shape with hollow core [142]. The three-dimensional metamaterials tubes are characterized as the THz wave propagates through the core of the tube. Figure 12(c) top, shows the device while Fig. 12(c) bottom shows the direction of THz wave for characterization. A tuning range of 50.6% within the frequency range of 0.75 - 1.13 *THz* was observed as the tube diameter decreases from 6.2 to 4.0 *mm*, as shown in Fig. 12(d). The blue-shift of the resonance frequency was attributed to the destructive magnetic interactions among the neighboring SRR unit cells on the increasingly curved surface. It was also found that if solid materials were inserted into the hollow tube core, the resonance frequency red-shifted due to the refractive index change, shown in Fig. 12 (e). Specifically, the permittivity of the inner core increases, leading to the red-shift in the resonance frequency. This way, the THz tube can be used to determine the unknown materials through the spectral signatures of the unknown materials. Refractive index changes as small as 0.0075 can be detect in conjunction with conventional THz-time-domain spectroscopy.

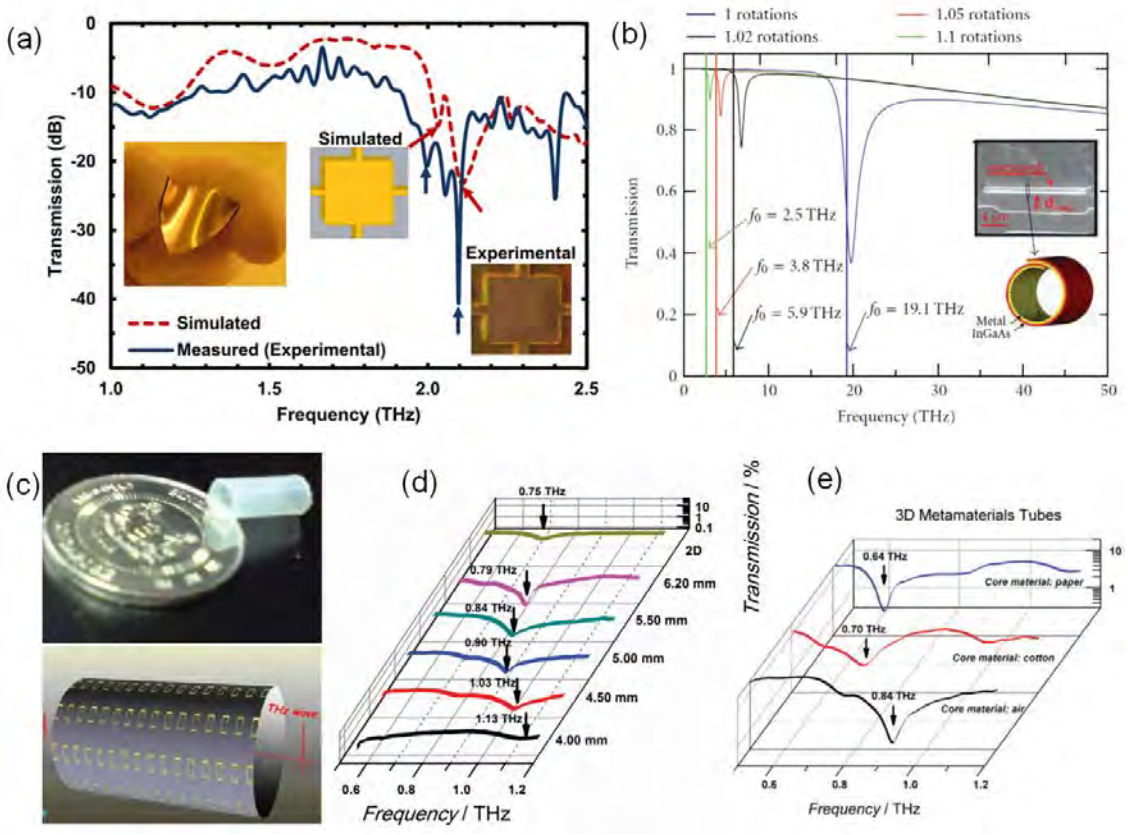

Fig. 12 (a) THz response of fishnet metamaterials on flexible PDMS substrate, inset: the device. Reprinted with permission from [140] Copyright [2012], American Institute of Physics. (b) Simulated responses of rolled-up THz metamaterials made of semiconductor materials, inset: the microroll. (copyright request submitted) (Copyright needs to be applied by publisher) (c) A 3D THz metamaterial tube, (d) and (e), tunable response with hollow and solid core, respectively.

6. Outlook

Metamaterials have entered a phase where they can be implemented into functional devices and no longer only serve as a study case of curious electromagnetic phenomena. The greatest impacts of metamaterials in technological world are yet to be felt, but with current pace of development, it will not be surprising to see practical metadevices in near future. This is especially realistic in the terahertz field, where the metamaterials fabrication is not as challenging as in optical domains. With the terahertz systems entering industrial setting, active tunable metamaterial devices are particularly desirable to raise the performance and functionality of terahertz systems in imaging, sensing, spectroscopy and non-destructive evaluation.

Acknowledgment.

This work was partially supported by A*STAR under grants No. 092 1540097.

References

[1] V. G. Veselago. "The electrodynamics of substances with simultaneously negative values [illegible] *Physics Uspekhi*, 10, 4, 509 (1968).

[2] D. R. Smith, W. J. Padilla, D. C. Vier, et. al. "Composite medium with simultaneously negative permeability and permittivity". *Physical Review Letters*, 84, 18, 4184-4187 (2000).

[3] D. R. Smith, S. Schultz, P. Markos, et. al. "Determination of effective permittivity and permeability of metamaterials from reflection and transmission coefficients". *Physical Review B*, 65, 19 (2002).

[4] D. R. Smith, J. B. Pendry, and M. C. K. Wiltshire. "Metamaterials and negative refractive index". *Science*, 305, 5685, 788-792 (2004).

[5] J. B. Pendry, A. J. Holden, D. J. Robbins, et. al. "Magnetism from conductors and enhanced nonlinear phenomena". *Ieee Transactions on Microwave Theory and Techniques*, 47, 11, 2075-2084 (1999).

[6] J. B. Pendry, D. Schurig, and D. R. Smith. "Controlling electromagnetic fields". *Science*, 312, 5781, 1780-1782 (2006).

[7] R. A. Shelby, D. R. Smith, and S. Schultz. "Experimental verification of a negative index of refraction". *Science*, 292, 5514, 77-79 (2001).

[8] C. M. Soukoulis, M. Kafesaki, and E. N. Economou. "Negative-index materials: New frontiers in optics". *Advanced Materials*, 18, 15, 1941-1952 (2006).

[9] A. A. Zharov, I. V. Shadrivov, and Y. S. Kivshar. "Nonlinear properties of left-handed metamaterials". *Physical Review Letters*, 91, 3 (2003).

[10] R. Marques, J. Martel, F. Mesa, et. al. "Left-handed-media simulation and transmission of EM waves in subwavelength split-ring-resonator-loaded metallic waveguides". *Physical Review Letters*, 89, 18 (2002).

[11] R. Marques, F. Mesa, J. Martel, et. al. "Comparative analysis of edge- and broadside-coupled split ring resonators for metamaterial design - Theory and experiments". *Ieee Transactions on Antennas and Propagation*, 51, 10, 2572-2581 (2003).

[12] H. O. Moser, B. D. F. Casse, O. Wilhelmi, et. al. "Terahertz response of a microfabricated rod-split-ring-resonator electromagnetic metamaterial". *Physical Review Letters*, 94, 6 (2005).

[13] C. M. Soukoulis, J. Zhou, T. Koschny, et. al. "The science of negative index materials". *Journal of Physics-Condensed Matter*, 20, 30 (2008).

[14] B. Pradarutti, C. Rau, G. Torosyan, et. al. "Plasmonic response in a one-dimensional periodic structure of metallic rods". *Applied Physics Letters*, 87, 20 (2005).

[15] J. B. Pendry, A. J. Holden, W. J. Stewart, et. al. "Extremely low frequency plasmons in metallic mesostructures". *Physical Review Letters*, 76, 25, 4773-4776 (1996).

[16] P. A. Belov, C. R. Simovski, and S. A. Tretyakov. "Two-dimensional electromagnetic crystals formed by reactively loaded wires". *Physical Review e*, 66, 3 (2002).

[17] S. Zhang, S. Qu, H. Ma, et. al. "Design and simulation of left-handed-property structure based on parallel metallic slabs". *Acta Physica Sinica*, 58, 6, 3961-3965 (2009).

[18] M. Kafesaki, I. Tsiapa, N. Katsarakis, et. al. "Left-handed metamaterials: The fishnet structure and its variations". *Physical Review B*, 75, 23 (2007).

[19] C. Menzel, T. Paul, C. Rockstuhl, et. al. "Validity of effective material parameters for optical fishnet metamaterials". *Physical Review B*, 81, 3 (2010).

[20] G. Dolling, M. Wegener, C. Soukoulis, et. al. "Design-related losses of double-fishnet negative-index photonic metamaterials". *Optics Express*, 15, 18, 11536-11541 (2007).

[21] A. Fang, T. Koschny, and C. Soukoulis. "Self-consistent calculations of loss-compensated fishnet metamaterials". *Physical Review B*, 82, 12 (2010).

[22] A. Minovich, D. N. Neshev, D. A. Powell, et. al. "Tilted response of fishnet metamaterials at near-infrared optical wavelengths". *Physical Review B*, 81, 11 (2010).

[23] R. Marques, L. Jelinek, F. Mesa, et. al. "Analytical theory of wave propagation through stacked fishnet metamaterials". *Optics Express*, 17, 14, 11582-11593 (2009).

[24] A. Mary, S. G. Rodrigo, L. Martin-Moreno, et. al. "Holey metal films: From extraordinary transmission to negative-index behavior". *Physical Review B*, 80, 16 (2009).

[25] P. Ding, E. Liang, W. Hu, et. al. "Numerical simulations of terahertz double-negative metamaterial with isotropic-like fishnet structure". *Photonics and Nanostructures-Fundamentals and Applications*, 7, 2, 92-100 (2009).

[26] J. Yang, C. Sauvan, H. Liu, et. al. "Theory of Fishnet Negative-Index Optical Metamaterials". *Physical Review Letters*, 107, 4 (2011).

[27] L. Jelinek, R. Marques, and J. Machac. "Fishnet Metamaterials - Rules for Refraction and Limits of Homogenization". *Optics Express*, 18, 17, 17940-17949 (2010).

[28] S. Zhang, Y. S. Park, J. Li, et. al. "Negative Refractive Index in Chiral Metamaterials". *Physical Review Letters*, 102, 2 (2009).

[29] J. Yao, Z. Liu, Y. Liu, et. al. "Optical negative refraction in bulk metamaterials of nanowires". *Science*, 321, 5891, 930 (2008).

[30] V. M. Shalaev. "Optical negative-index metamaterials". *Nature Photonics*, 1, 1, 41-48 (2007).

[31] V. M. Shalaev, W. S. Cai, U. K. Chettiar, et. al. "Negative index of refraction in optical metamaterials". *Optics Letters*, 30, 24, 3356-3358 (2005).

[32] E. Kim, Y. Shen, W. Wu, et. al. "Modulation of negative index metamaterials in the near-IR range". *Applied Physics Letters*, 91, 17 (2007).

[33] G. Dolling, C. Enkrich, M. Wegener, et. al. "Low-loss negative-index metamaterial at telecommunication wavelengths". *Optics Letters*, 31, 12, 1800-1802 (2006).

[34] J. Hao, L. Zhou, and M. Qiu. "Nearly total absorption of light and heat generation by plasmonic metamaterials". *Physical Review B*, 83, 16 (2011).

[35] M. Li, H. Yang, X. Hou, et. al. "Perfect Metamaterial Absorber with Dual Bands". *Progress in Electromagnetics Research-Pier*, 108, 37-49 (2010).

[36] Y. Cheng, H. Yang, Z. Cheng, et. al. "Perfect metamaterial absorber based on a split-ring-cross resonator". *Applied Physics A-Materials Science & Processing*, 102, 1, 99-103 (2011).

[37] N. Landy, I, S. Sajuyigbe, J. Mock, et. al. "Perfect metamaterial absorber". *Physical Review Letters*, 100, 20 (2008).

[38] J. B. Pendry. "Negative refraction makes a perfect lens". *Physical Review Letters*, 85, 18, 3966-3969 (2000).

[39] I. I. Smolyaninov, Y. J. Hung, and C. C. Davis. "Magnifying superlens in the visible frequency range". *Science*, 315, 5819, 1699-1701 (2007).

[40] N. Fang and X. Zhang. "Imaging properties of a metamaterial superlens". *Applied Physics Letters*, 82, 2, 161-163 (2003).

[41] N. Fang, Z. W. Liu, T. J. Yen, et. al. "Regenerating evanescent waves from a silver superlens". *Optics Express*, 11, 7, 682-687 (2003).

[42] S. Zhang, L. Yin, and N. Fang. "Focusing Ultrasound with an Acoustic Metamaterial Network". *Physical Review Letters*, 102, 19 (2009).

[43] K. Aydin, I. Bulu, and E. Ozbay. "Subwavelength resolution with a negative-index metamaterial superlens". *Applied Physics Letters*, 90, 25 (2007).

[44] H. Lee, Z. Liu, Y. Xiong, et. al. "Development of optical hyperlens for imaging below the diffraction limit". *Optics Express*, 15, 24, 15886-15891 (2007).

[45] K. Aydin, I. Bulu, and E. Ozbay. "Focusing of electromagnetic waves by a left-handed metamaterial flat lens". *Optics Express*, 13, 22, 8753-8759 (2005).

[46] H. Lee, Y. Xiong, N. Fang, et. al. "Realization of optical superlens imaging below the diffraction limit". *New Journal of Physics*, 7 (2005).

[47] F. Mesa, M. J. Freire, R. Marques, et. al. "Three-dimensional superresolution in metamaterial slab lenses: Experiment and theory". *Physical Review B*, 72, 23 (2005).

[48] W. Lu and S. Sridhar. "Superlens imaging theory for anisotropic nanostructured metamaterials with broadband all-angle negative refraction". *Physical Review B*, 77, 23 (2008).

[49] N. Fang, H. Lee, C. Sun, et. al. "Sub-diffraction-limited optical imaging with a silver superlens". *Science*, 308, 5721, 534-537 (2005).

[50] A. V. Kildishev and V. M. Shalaev. "Engineering space for light via transformation optics". *Optics Letters*, 33, 1, 43-45 (2008).

[51] Y. Liu, T. Zentgraf, G. Bartal, et. al. "Transformational Plasmon Optics". *Nano Letters*, 10, 6, 1991-1997 (2010).

[52] A. Kildishev, V, W. Cai, U. Chettiar, et. al. "Transformation optics: approaching broadband electromagnetic cloaking". *New Journal of Physics*, 10 (2008).

[53] P. Tichit, S. Burokur, and A. de Lustrac. "Ultradirective antenna via transformation optics". *Journal of Applied Physics*, 105, 10 (2009).

[54] D. H. Kwon and D. H. Werner. "Transformation Electromagnetics: An Overview of the Theory and Applications". *Ieee Antennas and Propagation Magazine*, 52, 1, 24-46 (2010).

[55] R. Liu, C. Ji, J. Mock, et. al. "Broadband Ground-Plane Cloak". *Science*, 323, 5912, 366-369 (2009).

[56] S. Xiao, V. P. Drachev, A. V. Kildishev, et. al. "Loss-free and active optical negative-index metamaterials". *Nature*, 466, 7307, 735-7U6 (2010).

[57] B. Wang, J. Zhou, T. Koschny, et. al. "Chiral metamaterials: simulations and experiments". *Journal of Optics A-Pure and Applied Optics*, 11, 11 (2009).

[58] Z. Wu, B. Zeng, and S. Zhong. "A Double-Layer Chiral Metamaterial with Negative Index". *Journal of Electromagnetic Waves and Applications*, 24, 7, 983-992 (2010).

[59] R. Singh, E. Plum, C. Menzel, et. al. "Terahertz metamaterial with asymmetric transmission". *Physical Review B*, 80, 15 (2009).

[60] V. Yannopapas. "Negative index of refraction in artificial chiral materials". *Journal of Physics-Condensed Matter*, 18, 29, 6883-6890 (2006).

[61] B. B. Hu and M. C. Nuss. "Imaging with Terahertz Waves". *Optics Letters*, 20, 16, 1716-& (1995).

[62] D. M. Mittleman, R. H. Jacobsen, and M. C. Nuss. "T-ray imaging". *Ieee Journal of Selected Topics in Quantum Electronics*, 2, 3, 679-692 (1996).

[63] D. M. Mittleman, M. Gupta, R. Neelamani, et. al. "Recent advances in terahertz imaging". *Applied Physics B-Lasers and Optics*, 68, 6, 1085-1094 (1999).

[64] J. F. Federici, B. Schulkin, F. Huang, et. al. "THz imaging and sensing for security applications - explosives, weapons and drugs". *Semiconductor Science and Technology*, 20, 7, S266-S280 (2005).

[65] M. C. Beard, G. M. Turner, and C. A. Schmuttenmaer. "Terahertz spectroscopy". *Journal of Physical Chemistry B*, 106, 29, 7146-7159 (2002).

[66] P. H. Siegel. "Terahertz technology in biology and medicine". *Ieee Transactions on Microwave Theory and Techniques*, 52, 10, 2438-2447 (2004).

[67] M. Brucherseifer, M. Nagel, P. H. Bolivar, et. al. "Label-free probing of the binding state of DNA by time-domain terahertz sensing". *Applied Physics Letters*, 77, 24, 4049-4051 (2000).

[68] M. C. Kemp, P. F. Taday, B. E. Cole, et. al. "Security applications of terahertz technology". *Terahertz for Military and Security Applications*, 5070, 44-52 (2003).

[69] W. L. Chan, J. Deibel, and D. M. Mittleman. "Imaging with terahertz radiation". *Reports on Progress in Physics*, 70, 8, 1325-1379 (2007).

[70] R. M. Woodward, B. E. Cole, V. P. Wallace, et. al. "Terahertz pulse imaging in reflection geometry of human skin cancer and skin tissue". *Physics in Medicine and Biology*, 47, 21, 3853-3863 (2002).

[71] D. Dragoman and M. Dragoman. "Terahertz fields and applications". *Progress in Quantum Electronics*, 28, 1, 1-66 (2004).

[72] H. T. Chen, R. Kersting, and G. C. Cho. "Terahertz imaging with nanometer resolution". *Applied Physics Letters*, 83, 15, 3009-3011 (2003).

[73] P. F. Taday, I. V. Bradley, D. D. Arnone, et. al. "Using terahertz pulse spectroscopy to study the crystalline structure of a drug: A case study of the polymorphs of ranitidine hydrochloride". *Journal of Pharmaceutical Sciences*, 92, 4, 831-838 (2003).

[74] P. Y. Han, M. Tani, M. Usami, et. al. "A direct comparison between terahertz time-domain spectroscopy and far-infrared Fourier transform spectroscopy". *Journal of Applied Physics*, 89, 4, 2357-2359 (2001).

[75] K. J. Siebert, H. Quast, R. Leonhardt, et. al. "Continuous-wave all-optoelectronic terahertz imaging". *Applied Physics Letters*, 80, 16, 3003-3005 (2002).

[76] D. M. Mittleman, R. H. Jacobsen, R. Neelamani, et. al. "Gas sensing using terahertz time-domain spectroscopy". *Applied Physics B-Lasers and Optics*, 67, 3, 379-390 (1998).

[77] X. C. Zhang. "Terahertz wave imaging: horizons and hurdles". *Physics in Medicine and Biology*, 47, 21, 3667-3677 (2002).

[78] E. Pickwell and V. Wallace. "Biomedical applications of terahertz technology". *Journal of Physics D-Applied Physics*, 39, 17, R301-R310 (2006).

[79] A. Dobroiu, M. Yamashita, Y. N. Ohshima, et. al. "Terahertz imaging system based on a backward-wave oscillator". *Applied Optics*, 43, 30, 5637-5646 (2004).

[80] C. J. Strachan, T. Rades, D. A. Newnham, et. al. "Using terahertz pulsed spectroscopy to study crystallinity of pharmaceutical materials". *Chemical Physics Letters*, 390, 1-3, 20-24 (2004).

[81] P. H. Siegel. "THz instruments for space". *Ieee Transactions on Antennas and Propagation*, 55, 11, 2957-2965 (2007).

[82] M. C. Gaidis, H. M. Pickett, C. D. Smith, et. al. "A 2.5-THz receiver front end for spaceborne applications". *Ieee Transactions on Microwave Theory and Techniques*, 48, 4, 733-739 (2000).

[83] M. Tonouchi. "Cutting-edge terahertz technology". *Nature Photonics*, 1, 2, 97-105 (2007).

[84] M. Beruete, M. Navarro-Cia, M. Sorolla, et. al. "Negative refraction through an extraordinary transmission left-handed metamaterial slab". *Physical Review B*, 79, 19 (2009).

[85] D. R. Smith, J. J. Mock, A. F. Starr, et. al. "Gradient index metamaterials". *Physical Review e*, 71, 3 (2005).

[86] H. T. Chen, W. J. Padilla, J. M. Zide, et. al. "Active terahertz metamaterial devices". *Nature*, 444, 7119, 597-600 (2006).

[87] H. T. Chen, J. F. O'Hara, A. J. Taylor, et. al."Complementary planar terahertz metamaterials". *Optics Express*, 15, 3, 1084-1095 (2007).

[88] M. Choi, S. H. Lee, Y. Kim, et. al. "A terahertz metamaterial with unnaturally high refractive index". *Nature*, 470, 7334, 369-373 (2011).

[89] B. Ferguson and X. C. Zhang. "Materials for terahertz science and technology". *Nature Materials*, 1, 1, 26-33 (2002).

[90] S. Linden, C. Enkrich, M. Wegener, et. al. "Magnetic response of metamaterials at 100 terahertz". *Science*, 306, 5700, 1351-1353 (2004).

[91] M. Seo, H. Park, S. Koo, et. al. "Terahertz field enhancement by a metallic nano slit operating beyond the skin-depth limit". *Nature Photonics*, 3, 3, 152-156 (2009).

[92] H. Tao, A. Strikwerda, K. Fan, et. al. "Reconfigurable Terahertz Metamaterials". *Physical Review Letters*, 103, 14 (2009).

[93] T. J. Yen, W. J. Padilla, N. Fang, et. al. "Terahertz magnetic response from artificial materials". *Science*, 303, 5663, 1494-1496 (2004).

[94] S. M. Spearing. "Materials issues in microelectromechanical systems (MEMS)". *Acta Materialia*, 48, 1, 179-196 (2000).

[95] J. J. Yao. "RF MEMS from a device perspective". *Journal of Micromechanics and Microengineering*, 10, 4, R9-R38 (2000).

[96] N. T. Nguyen, X. Y. Huang, and T. K. Chuan. "MEMS-micropumps: A review". *Journal of Fluids Engineering-Transactions of the Asme*, 124, 2, 384-392 (2002).

[97] E. Verpoorte and N. F. De Rooij. "Microfluidics meets MEMS". *Proceedings of the Ieee*, 91, 6, 930-953 (2003).

[98] S. Trolier-McKinstry and P. Muralt. "Thin film piezoelectrics for MEMS". *Journal of Electroceramics*, 12, 1-2, 7-17 (2004).

[99] Y. P. Zhao, L. S. Wang, and T. X. Yu. "Mechanics of adhesion in MEMS - a review". *Journal of Adhesion Science and Technology*. 17, 4, 519-546 (2003).

[100] M. Mehregany, C. A. Zorman, N. Rajan, et. al. "Silicon carbide MEMS for harsh environments". *Proceedings of the Ieee*, 86, 8, 1594-1610 (1998).

[101] A. C. R. Grayson, R. S. Shawgo, A. M. Johnson, et. al. "A BioMEMS review: MEMS technology for physiologically integrated devices". *Proceedings of the Ieee*, 92, 1, 6-21 (2004).

[102] Y. Huang, E. L. Mather, J. L. Bell, et. al. "MEMS-based sample preparation for molecular diagnostics". *Analytical and Bioanalytical Chemistry*, 372, 1, 49-65 (2002).

[103] C. M. Ho and Y. C. Tai. "Review: MEMS and its applications for flow control". *Journal of Fluids Engineering-Transactions of the Asme*, 118, 3, 437-447 (1996).

[104] D. P. Arnold. "Review of microscale magnetic power generation". *Ieee Transactions on Magnetics*, 43, 11, 3940-3951 (2007).

[105] L. Y. Lin and E. L. Goldstein. "Opportunities and challenges for MEMS in lightwave communications". *Ieee Journal of Selected Topics in Quantum Electronics*, 8, 1, 163-172 (2002).

[106] A. bbaspour-Tamijani, L. Dussopt, and G. M. Rebeiz. "Miniature and tunable filters using MEMS capacitors". *Ieee Transactions on Microwave Theory and Techniques*, 51, 7, 1878-1885 (2003).

[107] C. L. Goldsmith, A. Malczewski, Z. J. Yao, et. al. "RF MEMs variable capacitors for tunable filters". *International Journal of Rf and Microwave Computer-Aided Engineering*, 9, 4, 362-374 (1999).

[108] A. Pothier, J. C. Orlianges, G. Z. Zheng, et. al. "Low-loss 2-bit tunable bandpass filters using MEMS DC contact switches". *Ieee Transactions on Microwave Theory and Techniques*, 53, 1, 354-360 (2005).

[109] W. D. Yan and R. R. Mansour. "Tunable dielectric resonator bandpass filter with embedded MEMS tuning elements". *Ieee Transactions on Microwave Theory and Techniques*, 55, 1, 154-160 (2007).

[110] E. Ekmekci, A. C. Strikwerda, K. Fan, et. al. "Frequency tunable terahertz metamaterials using broadside coupled split-ring resonators". *Physical Review B*, 83, 193103 (2011).

[111] W. M. Zhu, A. Q. Liu, X. M. Zhang, et. al. "Switchable Magnetic Metamaterials Using Micromachining Processes". *Advanced Materials*, 23, 15, 1792-+ (2011).

[112] W. Zhang, A. Liu, W. Zhu, et. al. "Micromachined switchable metamaterial with dual resonance". *Applied Physics Letters*, 101, 15 (2012).

[113] W. Zhu, A. Liu, W. Zhang, et. al. "Polarization dependent state to polarization independent state change in THz metamaterials". *Applied Physics Letters*, 99, 22 (2011).

[114] W.M.Zhu, A.Q.Liu, T.Bourouina, et. al."Microelectromechanical Maltese-cross metamaterial with tunable terahertz anisotropy". *Nature Communications*, 3, 1274 (2012).

[115] W.M.Zhu, A.Q.Liu, T.Bourouina, et. al."Microelectromechanical Maltese-cross metamaterial with tunable terahertz anisotropy". *Nature Communications*, 3, 1274 (2012).

[116] H. Tao, A. C. Strikwerda, K. Fan, et. al. "MEMS Based Structurally Tunable Metamaterials at Terahertz Frequencies". *Journal of Infrared Millimeter and Terahertz Waves*, 32, 5, 580-595 (2011).

[117] B. Ozbey and O. Aktas. "Continuously tunable terahertz metamaterial employing magnetically actuated cantilevers". *Optics Express*, 19, 7, 5741-5752 (2011).

[118] W. P. Taylor, O. Brand, and M. G. Allen. "Fully integrated magnetically actuated micromachined relays". *Journal of Microelectromechanical Systems*, 7, 2, 181-191 (1998).

[119] L. Chang and W. Y. Yong. "Micromachined magnetic actuators using electroplated permalloy". *Ieee Transactions on Magnetics*, 35, 3, 1976-1985 (1999).

[120] N. H. Shen, M. Kafesaki, T. Koschny, et. al. "Broadband blueshift tunable metamaterials and dual-band switches". *Physical Review B*, 79, 16 (2009).

[121] D. Shrekenhamer, S. Rout, A. C. Strikwerda, et. al. "High speed terahertz modulation from metamaterials with embedded high electron mobility transistors". *Optics Express*, 19, 10, 9968-9975 (2011).

[122] W. L. Chan, H. T. Chen, A. J. Taylor, et. al. "A spatial light modulator for terahertz beams". *Applied Physics Letters*, 94, 21 (2009).

[123] X. Shen and T. J. Cui. "Photoexcited broadband redshift switch and strength modulation of terahertz metamaterial absorber". *Journal of Optics*, 14, 11 (2012).

[124] S. A. Maier, S. R. Andrews, L. Martin-Moreno, et. al. "Terahertz surface plasmon-polariton propagation and focusing on periodically corrugated metal wires". *Physical Review Letters*, 97, 17 (2006).

[125] J. B. Pendry, L. Martin-Moreno, and F. J. Garcia-Vidal. "Mimicking surface plasmons with structured surfaces". *Science*, 305, 5685, 847-848 (2004).

[126] P. Andrew and W. L. Barnes. "Energy transfer across a metal film mediated by surface plasmon polaritons". *Science*, 306, 5698, 1002-1005 (2004).

[127] E. Litwinstaszewska, W. Szymanska, and R. Piotrzkowski. "The Electron-Mobility and Thermoelectric-Power in Insb at Atmospheric and Hydrostatic Pressures". *Physica Status Solidi B-Basic Research*, 106, 2, 551-559 (1981).

[128] V. Giannini, A. Berrier, S. A. Maier, et. al. "Scattering efficiency and near field enhancement of active semiconductor plasmonic antennas at terahertz frequencies". *Optics Express*, 18, 3, 2797-2807 (2010).

[129] S. Hanham, A. Fernandez-Dominguez, I, J. Teng, et. al. "Broadband Terahertz Plasmonic Response of Touching InSb Disks". *Advanced Materials*, 24, 35, OP226-OP230 (2012).

[130] L. Y. Deng, J. H. Teng, H. Y. Liu, et. al. "Direct Optical Tuning of Terahertz Plasmonic Response of InSb Subwavelength Gratings". *Advanced Optical Materials*, (2012). accepted

[131] K. S. Novoselov, A. K. Geim, S. V. Morozov, et. al. "Electric field effect in atomically thin carbon films". *Science*, 306, 5696, 666-669 (2004).

[132] F. Bonaccorso, Z. Sun, T. Hasan, et. al. "Graphene photonics and optoelectronics". *Nature Photonics*, 4, 9, 611-622 (2010).

[133] A. Geim. "Graphene: Status and Prospects". *Science*, 324, 5934, 1530-1534 (2009).

[134] A. Geim and K. Novoselov. "The rise of graphene". *Nature Materials*, 6, 3, 183-191 (2007).

[135] B. Wang, X. Zhang, Yuan.X., et. al. "Negative Coupling and Directional Splitting of Surface Plasmons in Monolayer Graphene Sheet Arrays". *Physical Review Letters*, 109, 073901 (2012).

[136] L. Ju, B. Geng, J. Horng, et. al. "Graphene plasmonics for tunable terahertz metamaterials". *Nature Nanotechnology*, 6, 10, 630-634 (2011).

[137] A. Vakil and N. Engheta. "Transformation Optics Using Graphene". *Science*, 332, 6035, 1291-1294 (2011).

[138] S. H. Lee, M. Choi, T. T. Kim, et. al. "Switching terahertz waves with gate-controlled active graphene metamaterials". *Nature Materials*, 11, 11, 936-941 (2012).

[139] H. Tao, A. Strikwerda, K. Fan, et. al. "Terahertz metamaterials on free-standing highly-flexible polyimide substrates". *Journal of Physics D-Applied Physics*, 41, 23 (2008).

[140] I. Khodasevych, C. Shah, S. Sriram, et. al. "Elastomeric silicone substrates for terahertz fishnet metamaterials". *Applied Physics Letters*, 100, 6 (2012).

[141] I. Semchenko, V, S. Khakhomov, E. Naumova, et. al. "Study of the properties of artificial anisotropic structures with high chirality". *Crystallography Reports*, 56, 3, 366-373 (2011).

[142] Z. Chen, M. Rahmani, Y. Gong, et. al. "Realization of Variable Three-Dimensional Terahertz Metamaterial Tubes for Passive Resonance Tunability". *Advanced Materials*, 24, 23, OP143-OP147 (2012).